

Simulation of C-CP Fiber-Based Air Filtration

Christopher L. Cox, Ph.D.¹, Philip J. Brown, Ph.D.¹, John C. Larzelere²

¹Clemson University, Clemson, South Carolina USA

²Naval Surface Warfare Center, Dahlgren Division, Dahlgren, Virginia USA

Correspondence to:

Christopher L. Cox, Ph.D., email: clcox@clemson.edu

ABSTRACT

The overall goal of this project is to develop High Efficiency Particulate Air (HEPA) filter media, using conventional fiber spinning techniques, with lower pressure drop than current media through the use of shaped fibers. Capillary-channeled polymer (C-CP) fibers are gaining interest for use in a range of separations applications. This paper focuses on modeling air filtration where the filter consists of C-CP fibers. A variety of numerical tools are being used in this effort, including a finite element flow solver and Brownian dynamics simulation. Aspects of these techniques in relation to the problem at hand will be described, and simulation results including comparisons to round-fiber filters will be presented. The primary result presented here is the significant difference in predicted pressure drop between a prototype C-CP filter and a round-fiber filter with equal total cross-sectional area.

INTRODUCTION

A variety of computer models for predicting particle collection in fibrous filters have been presented in the literature. These simulations range from studying collection on a single fiber to particle separation in three-dimensional fibrous structures [1-5]. The majority of these efforts assume the fibers are round, though some have considered square or rectangular fibers [6-7].

The main goals in filter design are to maximize the collection efficiency and keep the pressure drop across the filter as low as possible [8]. By definition, High Efficiency Particulate Air (HEPA) filters have an efficiency of at least 99.97 percent for particles 0.3 microns or larger. This higher efficiency is also normally associated with a higher pressure drop, resulting in more work to push air through the filter media. The challenge in filter manufacturing is to meet efficiency standards while minimizing pressure drop across the filter in order to maximize the filter lifetime.

The mechanisms by which a particle is separated from a fluid stream are interception, inertial impaction, Brownian diffusion, and electrostatic capture, [8]. The effect of each mechanism is determined by several factors including particle size, fiber size, and fiber material (e.g. glass vs. synthetic). It has been recognized that fiber geometry can influence filter performance, though the filtration industry has been slow to exploit this potential improvement, [8].

This paper presents a simulation of depth filtration of airborne particles, where the filter is composed of 4DGTM polymer fibers. These deep-grooved fibers (also referred to as capillary-channeled polymer fibers) were developed by the Eastman Chemical Company. The technology was subsequently donated to the Clemson University Research Foundation. A scanning electron microscope image of a 4DGTM polyester fiber cross section, magnified 1000 times, is shown in Figure 1.

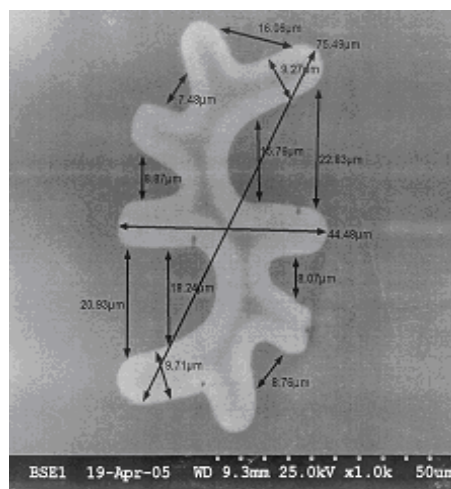


FIGURE 1. Cross section of 4DGTM C-CP fiber

The surface area of this fiber is approximately 2.5 times that of a round fiber of the same denier [8].

The rest of this paper is organized as follows. In the next section the mathematical models for the airflow and particle motion are described, along with solution methodology. Then modeling results are presented. The paper concludes with a summary and brief discussion of plans for continuing work.

MODEL DEVELOPMENT

Governing Equations

The fluid flow governing equations which we are using are the Stokes equations, found for example in Rief, et al. [5]. Written in dimensionless form the equations are:

$$-\Delta \mathbf{u} + \nabla p = \mathbf{0} \quad \text{in } \Omega \quad (1)$$

$$\text{div } \mathbf{u} = 0 \quad \text{in } \Omega \quad (2)$$

$$\mathbf{u} = 0 \quad \text{on } \Gamma_{\text{fiber}} \quad (3)$$

where Ω is the domain exterior to the fiber boundary Γ_{fiber} . These equations are applicable under the assumptions that the Reynolds number is low enough so that the incompressible Stokes equations are valid, and that the flow along the fiber surface satisfies a ‘no-slip’ condition. The equations are nondimensionalized using the face velocity, U , fluid viscosity, μ , and a characteristic length, L . The dimensionless dependent variables p (pressure) and \mathbf{u} (velocity), and independent variables (x, y) are related to the physical quantities by the equations

$$\begin{aligned} \mathbf{u}_{\text{phys}} &= U\mathbf{u}, & p_{\text{phys}} &= (\mu U/L)p \\ (x_{\text{phys}}, y_{\text{phys}}) &= (Lx, Ly) \end{aligned}$$

The fibers are assumed to be oriented parallel to one another, allowing for a two-dimensional simulation of the flow over the fiber cross sections. The domain is shown in Figure 2. The overall dimensions of this computational cell are approximately 200 microns in each direction. Each fiber has a maximum cross-sectional width of approximately 60 microns. The inflow and outflow dimensionless velocities (corresponding to boundaries Γ_{in} and Γ_{out} , respectively), are set to the nondimensionalized face velocity, which is 1. Fully periodic boundary conditions are imposed on the sides of the domain, denoted Γ_{upper} and Γ_{lower} [9]. Since only the gradient of pressure appears in equation (1), for uniqueness the pressure must be specified at a point in the

domain. In this simulation, $p = 0$ at a point on Γ_{in} . In summary, the fluid flow boundary conditions are:

$$\mathbf{u} = \mathbf{0} \quad \text{on } \Gamma_{\text{fiber}} \quad (4)$$

$$\mathbf{u} = \begin{bmatrix} 1 \\ 0 \end{bmatrix} \quad \text{on } \Gamma_{\text{in}}, \Gamma_{\text{out}} \quad (5)$$

$$\mathbf{u}(\Gamma_{\text{upper}}) = \mathbf{u}(\Gamma_{\text{lower}}) \quad (6)$$

$$p(\Gamma_{\text{upper}}) = p(\Gamma_{\text{lower}}) \quad (7)$$

The periodic boundary conditions are more realistic than other conditions as they indicate that the computational cell in Figure 2 is part of a larger domain of repeated units, as shown in Figure 3.

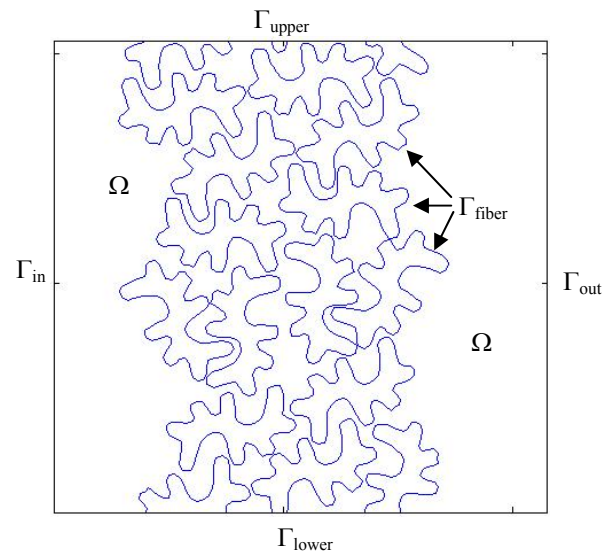


FIGURE 2. Solution domain.

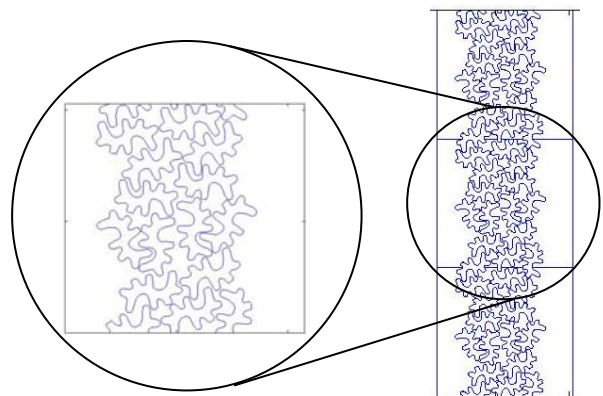


FIGURE 3. Computational cell and multiple cells

The fluid flow equations and the equation for particle motion are solved in decoupled fashion, assuming

that the particles are of low enough concentration and size so that the fluid motion is not affected by the presence of suspended particles. It is also assumed that the particles do not collide with one another.

The approach in Oh, et al. is used to model particle motion [1]. Given the fluid velocity field, the simulation of particle motion begins with a Langevin equation which in this case takes the form

$$\frac{d\mathbf{v}}{dt} = \beta(\mathbf{u} - \mathbf{v}) + \frac{\mathbf{F}_E}{m} + \mathbf{A}(t) \quad (8)$$

where \mathbf{v} is particle velocity, \mathbf{u} is the fluid (air) velocity, β is a friction coefficient, \mathbf{F}_E is the external force acting on the particle, including electric forces and gravity, and $\mathbf{A}(t)$ is random Brownian acceleration. In this paper the external force term is set to zero, and β is specified as

$$\beta = \frac{6\pi\mu r_p}{c_s m}$$

where r_p and m are particle radius and mass, respectively. Also, c_s is the Cunningham slip correction factor, given for air as

$$c_s = 1 + \frac{\lambda}{r_p} \left(A_1 + A_2 e^{-\frac{A_3 r_p}{\lambda}} \right)$$

where λ is the mean free path, $A_1 = 1.257$, $A_2 = 0.400$, and $A_3 = 0.55$ [10]. Integrating (8) over a very short time interval, on which the fluid velocity is assumed constant yields equation (9) for the particle velocity [1].

$$\mathbf{v} = \mathbf{v}_0 e^{-\beta t} + \mathbf{u}(1 - e^{-\beta t}) + \mathbf{R}_v(t) \quad (9)$$

In (9), $\mathbf{v}_0 = \mathbf{v}(0)$ and

$$\mathbf{R}_v(t) = \int_0^t e^{\beta(s-t)} \mathbf{A}(s) ds.$$

Replacing \mathbf{v} in (9) with $d\mathbf{r}/dt$ and integrating, along with imposing the condition $\mathbf{r}(0) = \mathbf{r}_0$, results in equation (10) for $\mathbf{r}(t)$.

$$\mathbf{r} = \mathbf{r}_0 + \frac{\mathbf{v}_0}{\beta} (1 - e^{-\beta t}) + \mathbf{u} \left[t - \frac{1}{\beta} (1 - e^{-\beta t}) \right] + \mathbf{R}_r(t) \quad (10)$$

The last term in (10) is

$$\mathbf{R}_r(t) = \int_0^t \left[\int_0^w e^{\beta s} \mathbf{A}(s) ds \right] e^{-\beta w} dw.$$

$\mathbf{R}_v(t)$ and $\mathbf{R}_r(t)$, which are random deviates generated from a bivariate Gaussian distribution, are calculated using equations (11)-(15).

$$\begin{bmatrix} \mathbf{R}_{vi} \\ \mathbf{R}_{ri} \end{bmatrix} = \begin{bmatrix} \sigma_{vi} & 0 \\ \sigma_{vri} / \sigma_{vi} & \left(\sigma_{ri}^2 - \sigma_{vri}^2 / \sigma_{vi}^2 \right)^{1/2} \end{bmatrix} \begin{bmatrix} n_i \\ m_i \end{bmatrix} \quad (11)$$

$$\sigma_{vi}^2 = \frac{q}{\beta} (1 - e^{-2\beta t}) \quad (12)$$

$$\sigma_{ri}^2 = \frac{q}{\beta^3} (2\beta t - 3 + 4e^{-\beta t} - e^{-2\beta t}) \quad (13)$$

$$\sigma_{vri} = \frac{q}{\beta^2} (1 - e^{\beta t})^2 \quad (14)$$

$$q = \frac{\beta k t}{m} \quad (15)$$

The normal distributions

$$N_i = \frac{1}{\sqrt{2\pi}} \int_{-\infty}^{n_i} e^{-s^2/2} ds$$

and

$$M_i = \frac{1}{\sqrt{2\pi}} \int_{-\infty}^{m_i} e^{-s^2/2} ds$$

where N_i and M_i are uniform random numbers between 0 and 1, are used to generate random numbers n_i and m_i . As in [1], equations (8) and (9) are solved for $\mathbf{v}(t)$ and $\mathbf{r}(t)$ using a sequence of time steps with Δt small enough so that fluid velocity can be assumed constant at each time step. Random numbers and random deviates needed for $\mathbf{A}(t)$ are calculated using the randlib.c package [11]. The random number generator uses an input character

string to generate a seed. We generate a random string from the computer clock time.

Numerical Solution

The boundary value problem consisting of equations (1)–(7) is solved using the finite element method. The finite element mesh is generated using the Triangle software package [12]. Figure 4 illustrates the mesh corresponding to the domain in Figure 2. In the Galerkin finite element formulation, continuous piecewise quadratic trial functions are used to approximate the components of \mathbf{u} and continuous piecewise linear functions are used to approximate p .

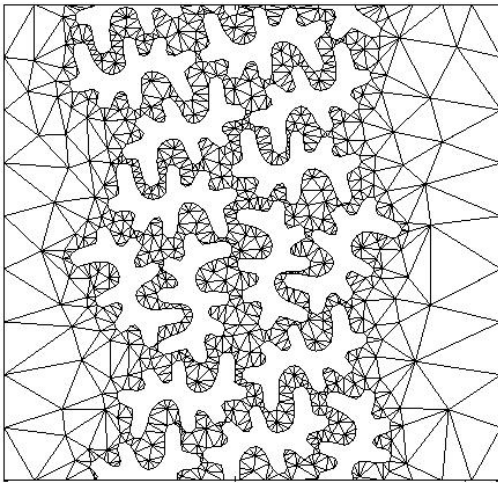


FIGURE 4. Finite element mesh generated by Triangle package.

Once the flow field is calculated, an ensemble of particle paths is generated. The algorithm for tracking the motion of a single particle is as follows:

For each particle:

- Initialize position at left boundary
- For each time step (while in interior):
 - Generate random numbers for Brownian motion terms
 - Update particle position and velocity
 - Determine triangle location of new position
 - Determine air velocity at new position

The particle positions are initialized at random locations along the inflow boundary. As in [1], for the first three time steps the horizontal component of the Brownian motion term is taken as the absolute value of the generated component to prevent the particle from escaping the cell through the inflow side. Particle capture (interception) occurs when the

particle is within one particle radius of the fiber surface.

RESULTS

The simulation code is written in the GCC C programming language [13]. Matlab is used for visualization [14]. The flow simulation takes approximately 20 minutes on a standard laptop or desktop computer. The particle simulations take roughly 1 second per particle. These CPU times depend on the complexity of the domain, density of the finite element mesh, and time step for the particle simulation.

For comparison, a round-fiber filter domain was constructed with the same number of fibers and identical fiber cross-sectional area as the C-CP filter. The round fiber domain and corresponding finite element mesh are displayed in Figure 5. Input parameters for the simulation are listed in Table 1. Figures 6 and 7 display the calculated pressure drop for the C-CP fiber filter and round fiber filter, respectively. Since the pressure is set at zero at a point on the inflow (left) boundary, the value of pressure on the outflow boundary is negative.

TABLE I. Parameter values used in calculations.

Face velocity	1.5 cm/s
Air viscosity	1.75×10^{-5} Pa·s
Number of particles	30
Particle diameter	0.15 μ
Particle density	1000 kg/m ³
Time step	2×10^{-7} s

As indicated by the color bars, the pressure drop through the C-CP fiber filter is less than half that of the round fiber filter.

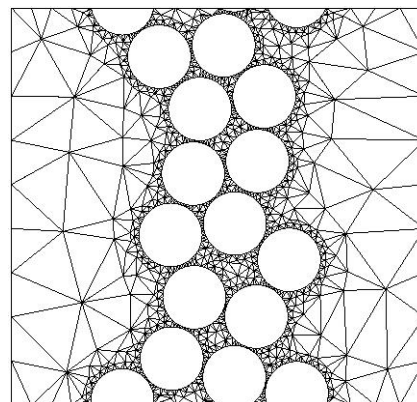


FIGURE 5. Finite element mesh for round fiber domain

Particle paths generated for each filter are displayed in Figures 8 and 9. In order to demonstrate the effect of the periodic boundary conditions, a red path color (rather than green) is used to identify those particles which exit through Γ_{upper} or Γ_{lower} and re-enter on the opposite side. Initial and terminal points for each particle are denoted with an open circle which is enlarged to be easily identified and therefore is not to scale. The results demonstrate that depth filtration (rather than surface or cake filtration) is taking place since particle capture is occurring throughout the domain. Strong conclusions about filtration efficiency are premature at this point, though it can be observed that fewer particles passed through the C-CP fiber filter.

CONCLUSIONS

This paper presents a proof of concept for simulation of air flow and particle collection in a filter composed of C-CP fibers. Comparison of results for a C-CP fiber filter with a round fiber filter indicate that a significantly less pressure drop occurs with the C-CP filter. Preliminary results for particle collection show that the C-CP filter is at least as efficient as the round fiber filter.

Next steps in this research are to include electrostatic effects in the particle motion simulation. The filter geometry will be extended to be more realistic (e.g. 6 to 8 layers). Filter efficiency studies will then be made, using averages over a large ensemble of model executions. Efforts to experimentally validate the model are underway. The model is sufficiently flexible to permit variations through the filter in fiber shape and size and particle size.

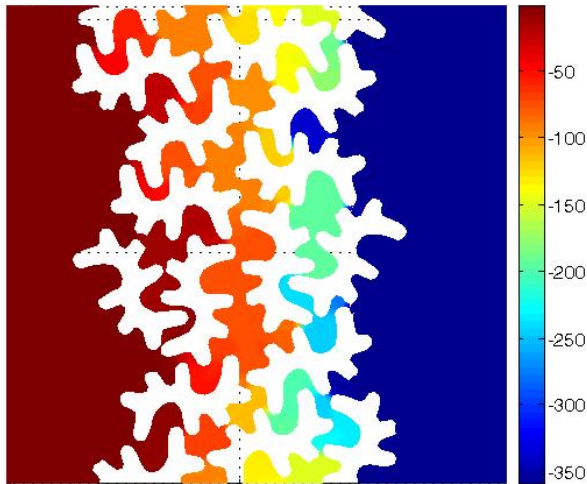


FIGURE 6. Pressure drop (Pa) for C-CP fiber filter

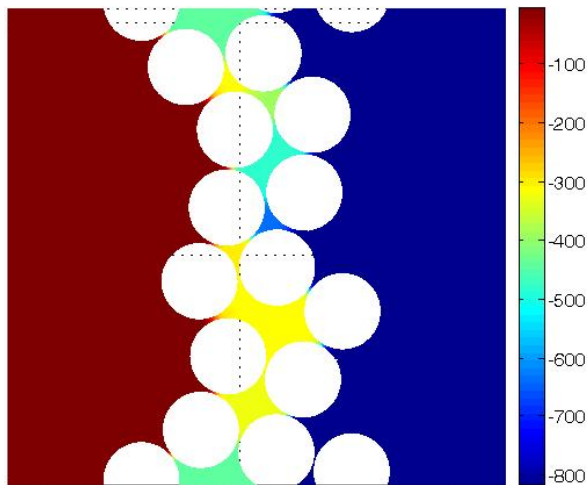


FIGURE 7. Pressure drop (Pa) for round fiber filter

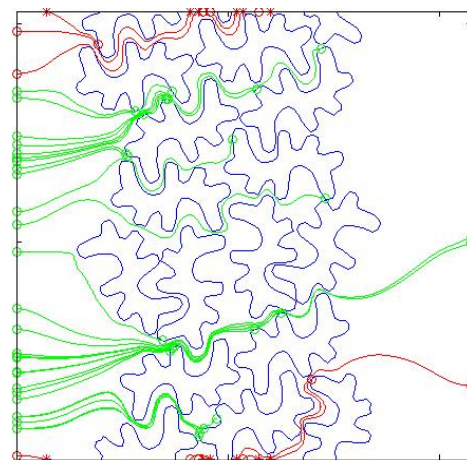


FIGURE 8. Particle paths for C-CP fiber filter

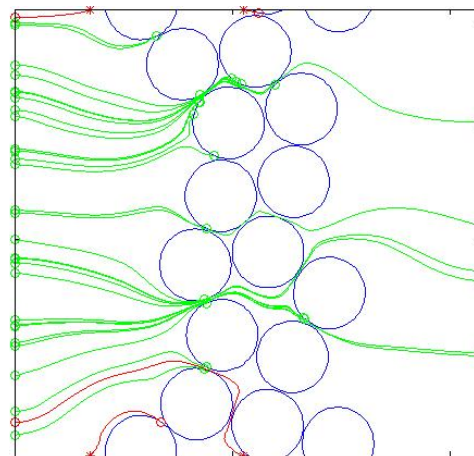


FIGURE 9. Particle paths for round fiber filter

Plans also call for incorporating the effect of particle build-up on the fiber surfaces, as well as generalization of this model to three-dimensions.

ACKNOWLEDGEMENT

This work was supported primarily by the US Defense Threat Reduction Agency, through the Naval Surface Warfare Center, Dahlgren Division, under Award Number BA07PRO035.

REFERENCES

- [1] Y-W Oh, K-J Joon, A-I Jung, and Y-W Jung, A simulation study on the collection of submicron particles in a unipolar charged fiber, *Aerosol Science and Technology*, 36: 573-582, 2002.
- [2] B.V. Ramarao, C. Tien, and S. Mohan, Calculation of single fiber efficiency for interception and impaction with superposed Brownian motion, *J. Aerosol Sci.*, 2:295-313, 1994.
- [3] A. Latz and A. Wiegmann, Simulation of fluid particle separation in realistic three dimensional fibre structures, *Proc. Filtech Europa Conference*, pp. 353-36, Düsseldorf, Germany, 2003.
- [4] Wiegmann, S. Rief, and A. Latz, Virtual material design and air filtration simulation techniques inside GeoDict and FilterDict, *Proc. AFS Annual Meeting*, Atlanta, USA, 2005.
- [5] S. Rief, A. Latz, and A. Wiegmann, Research note: Computer simulation of air filtration including electric surface charges in 3-dimensional fibrous microstructures, *Filtration*, Number 2, Volume 6, 2006, pp 169-172.
- [6] K. Adamiak, Aerosol deposition on an arbitrarily oriented single rectangular fiber in a uniform electric field, *Proc. IEEE-IAS Annual Meeting*, Lake Buena Vista, FL, vol. 2, pp. 1385-1389, 1995.
- [7] K. Adamiak, Viscous flow model for charged particle trajectories around a single square fiber in an electric field, *IEEE Transactions on industry applications*, vol. 35, no. 2, 352-358, 1999.
- [8] E. Vaughn and G. Ramachandran, Fiberglass vs. synthetic air filtration media, *INJ*, Fall, 41-53, 2002.

- [9] G. Segal, K. Vuik, and K. Kaasls, On the implementation of symmetric and antisymmetric periodic boundary conditions for incompressible flow, *International Journal for Numerical Methods in Fluids*, Vol. 18, 1153-1165, 1994.
- [10] N. Davies, *Air Filtration*. New York: Academic, 1973.
- [11] randlib.c is open source software which can be downloaded from several websites, including <ftp://ftp.jp.netbsd.org/pub/NetBSD/packages/distfiles/randlib-1.3/randlib.c-1.3.tar.gz>
- [12] J. R. Shewchuk, Triangle: engineering a 2D quality mesh generator and Delaunay triangulator, in *Applied Computational Geometry: Towards Geometric Engineering* (Ming C. Lin and Dinesh Manocha, editors), volume 1148 of *Lecture Notes in Computer Science*, pages 203-222, Springer-Verlag, Berlin, May 1996.
- [13] GCC, The GNU Compiler Collection, <http://gcc.gnu.org/>.
- [14] Matlab, www.mathworks.com.

AUTHORS' ADDRESSES

Christopher L. Cox, Ph.D.

Department of Mathematical Sciences
Clemson University
Clemson, SC 29634-0975
USA

Philip J. Brown, Ph.D.

School of Materials Science and Engineering
Clemson University
Clemson, SC 29634-0971
USA

John C. Larzelere

Naval Surface Warfare Center
Dahlgren Division
Dahlgren, VA
USA